Scientific Research Publishing

Advances in Materials Physics and Chemistry, 2024, 14, 213-234
https://www.scirp.org/journal/ampc
ISSN Online: 2162-5328
ISSN Print: 2162-531X

Molecular Dynamics, Physical Properties, Diffusion Coefficients and Activation Energy of the Lithium Oxide (Li-O) and Sodium Oxide (Na-O) Electrolyte (Cathode)

Alain Second Dzabana Honguelet[1,2,3*], Abel Dominique Eboungabeka[1,2], Timothée Nsongo[1,2,4]

[1]Faculty of Science and Technology, Marien Ngouabi University, Brazzaville, Congo
[2]Research Group on Physical, Chemical and Mineralogical Properties of Materials, Brazzaville, Congo
[3]Alpha Sciences and Beta Technologies Association, Brazzaville, Congo
[4]Geological and Mining Research Center, Brazzaville, Congo
Email: *second_alain@yahoo.fr, abeleboungabeka@gmail.com

How to cite this paper: Honguelet, A.S.D., Eboungabeka, A.D. and Nsongo, T. (2024) Molecular Dynamics, Physical Properties, Diffusion Coefficients and Activation Energy of the Lithium Oxide (Li-O) and Sodium Oxide (Na-O) Electrolyte (Cathode). *Advances in Materials Physics and Chemistry*, **14**, 213-234.
https://doi.org/10.4236/ampc.2024.149016

Received: September 2, 2024
Accepted: September 24, 2024
Published: September 27, 2024

Abstract

This work is a simulation model with the LAMMPS calculation code of an electrode based on alkali metal oxides (lithium, sodium and potassium) using the Lennard Jones potential. For a multiplicity of 8*8*8, we studied a gap-free model using molecular dynamics. Physical quantities such as volume and pressure of the Na-O and Li-O systems exhibit similar behaviors around the thermodynamic ensembles NPT and NVE. However, for the Na_2O system, at a minimum temperature value, we observe a range of total energy values; in contrast, for the Li_2O system, a minimum energy corresponds to a range of temperatures. Finally, for physicochemical properties, we studied the diffusion coefficient and activation energy of lithium and potassium oxides around their melting temperatures. The order of magnitude of the diffusion coefficients is given by the relation $D_{li\text{-}O} > D_{Na\text{-}O}$ for the multiplicity 8*8*8, while for the activation energy, the order is well reversed $Ea_{Na\text{-}O} > Ea_{Li\text{-}O}$.

Keywords

Molecular Dynamics, Diffusion Coefficients, Activation Energy, Lithium Oxide, Sodium Oxide, Lennard Jones Potential, Data File, Atomic and Charge Models, Cathode, LAMMPS

1. Introduction

Lithium batteries are widely used in electronic devices such as cell phones and

electric vehicles [1]. Studies are continuing to increase their efficiency and stability; computational models can be used to analyze lithium battery materials [2]. Recent studies establish the link between thermal conductivity and the diffusion coefficient and activation energy of electrolytes [3].

Nowadays, the use of lithium at the negative electrode, combined with a carefully chosen cathode (high potential), results in the highest mass energy values and a much higher voltage of the order of 4 V, compared with alkaline batteries of the order of 1.5 V [4] [5].

However, the use of lithium as a negative electrode requires specific safety devices and instructions for transport, use and recycling [6]. The implementation of a battery includes the installation of a depressurization cap (to prevent explosion following a pressure rise), electrical devices to prevent excessively high discharge rates (an element called a PTC, which is connected in series and whose electrical resistance increases with temperature), or accidental recharging (diode), or a rise in temperature (stop of discharge by breaker) [7]. Among the many existing systems, three families of lithium batteries can be distinguished, depending on the nature of the cathode and electrolyte used: liquid cathode batteries, solid cathode batteries and solid electrolyte batteries [8]. To address this lithium-related problem, we thought we'd look at alkali metals close to lithium [9].

Batteries are not new to the Physico-Chemical Properties of Materials research group; alumni have already carried out a practical study using basic solutions to obtain electrical energy [10]. They have also been studied at the Faculté des Sciences et Techniques in Congo Brazzaville in previous years [11].

In our previous study on batteries, based on the simulation of an electrochemical cell, we compared the properties of the lithium anode with those of neighboring alkali metals such as potassium and sodium; we also compared the activation energies of systems without vacancies with those of systems with vacancies in the center of the mesh for any multiplicities [12].

The present study is a simulation under the LAMMPS calculation code focused on the study of oxide electrolytes of the alkali metals Li-O, Na-O and K-O used as cathodes to complement our previous study based on the lithium anode.

2. Method

2.1. Molecular Dynamics

Molecular dynamics is a formidable tool for investigating matter at the atomic scale. It consists of numerically simulating the evolution of a system of particles as a function of time, with the aim of predicting and understanding experimental results [13]. It can reveal structural arrangements or dynamic phenomena that are still inaccessible to current experimental observation methods (EXAFS, NMR, Atom Probe Tomography - APT), especially with regard to amorphous materials such as glasses [14]. This move into the digital world requires time discretization to solve the Newtonian equations governing the motion of each particle [15].

The principle of molecular dynamics is then to integrate these discretized

equations under various physical constraints, using various algorithms that can be found in reference books such as Griebel *et al.* [16], a clear work containing examples and practical applications, useful for those wishing to start writing their own molecular dynamics program.

The methods presented are those used in this thesis. After an explanation of the *Velocity-Störmer-Verlet* algorithm, a balance between robustness, practicality and performance, a presentation of the Nosé-Hoover thermostat and barostat shows how temperature and pressure control of a material can be achieved in a fully integrated way [17]-[19].

A key point in simulations is the appropriate parameterization of interatomic interactions. The interaction potential used must first and foremost account for properties that are known in order to predict those that are not or to explain a phenomenon that is still poorly understood [20].

Calculating these interactions during simulation, particularly electrostatic interactions, is the most resource-intensive step in numerical computation. The method developed by Wolf overcomes this limitation, opening up the field of simulation to much larger size and time scales [21].

These methods and algorithms are eventually applied to the modeling of silica materials, in particular glasses, where certain properties and experimental behaviors are reproduced with acuity [22] [23].

2.1.1. Integration Algorithms for Newton's Equations

In classical molecular dynamics, each particle is considered as a point mass interacting at a distance with the others via an effective interaction potential [24]. In an ensemble of N interacting particles, the motion of particle i of mass m_i (with i = 1 to N) is governed by Equation (1):

$$m_i \frac{\mathrm{d}^2 x_i}{\mathrm{d}t^2} = F_i \tag{1}$$

With the convention $x_i = \vec{x}_i$ for the position vector, and F_i is the vector resulting from all the forces applied to particle i [25].

2.1.2. Standard Störmer-Verlet Method

The equations of motion are solved using the standard Störmer-Verlet method, which discretizes Newton's equations to determine particle positions and velocities over time. This method is essential for the numerical integration of the equations of motion [26].

The basic numerical method for solving the equations of motion is to perform a 3rd-order Taylor series expansion of position x around date t, *i.e.* at $t \pm \delta t$ (with δt small), see Equations (2) and (3):

$$t \pm \begin{cases} x(t+\delta t) = x(t) + \delta t \dfrac{\mathrm{d}x}{\mathrm{d}t} + \dfrac{1}{2}\delta t^2 \dfrac{\mathrm{d}^2 x}{\mathrm{d}t^2} + \dfrac{1}{6}\delta t^3 \dfrac{\mathrm{d}^3 x}{\mathrm{d}t^3} & (2) \\ x(t-\delta t) = x(t) - \delta t \dfrac{\mathrm{d}x}{\mathrm{d}t} + \dfrac{1}{2}\delta t^2 \dfrac{\mathrm{d}^2 x}{\mathrm{d}t^2} - \dfrac{1}{6}\delta t^3 \dfrac{\mathrm{d}^3 x}{\mathrm{d}t^3} & (3) \end{cases}$$

By adding and grouping the terms, we obtain Equation (4):

$$\frac{\mathrm{d}^2x}{\mathrm{d}t^2}=\frac{1}{\delta t^2}\left[x\left(t+\delta t\right)-2x\left(t\right)+x\left(t-\delta t\right)\right] \tag{4}$$

We discretize time using a time step δt (of the order of femtoseconds in Molecular Dynamics). At iteration n, the date is expressed by $t_n=n\delta t$, the position vector by x_i^n, the velocity vector by v_i^n and the force vector by F_i^n. After this discretization and digitization, the previous equation becomes, for the date $t_{n+1}=t_n+\delta t$, see Equation (5):

$$m_i\frac{1}{\delta t^2}\left(x_i^{n+1}-2x_i^n+x_i^{n-1}\right)=F_i^n \tag{5}$$

In the same way, but subtracting the terms this time, we obtain the velocity expression:

$$\frac{\mathrm{d}^2x}{\mathrm{d}t^2}=\frac{x\left(t+\delta t\right)-x\left(t-\delta t\right)}{2\delta t}=v_i^n=\frac{x_i^{n+1}-x_i^{n-1}}{2\delta t} \tag{6}$$

This is the standard form of the Störmer-Verlet method for integrating Newton's equations:

$$\begin{cases} x_i^{n+1}=2x_i^n-x_i^{n-1}+\dfrac{\delta t^2}{m_i}F_i^n & (7)\\ v_i^n=\dfrac{x_i^{n+1}-x_i^{n-1}}{2\delta t} & (8)\end{cases}$$

2.2. Work Procedure

In this section, we present our approach to simulating our stack and calculating activation energies. We paid particular attention to the choice of elements, the various interactions between systems, and the composition of the systems.

The program is a LAMMPS script that simulates a sodium-oxygen system at the atomic scale using molecular dynamics methods. It sets up a 3D simulation with periodic boundary conditions ('boundary p p p') and metal units ('units metal'). The atom style includes electric charges ('atom_style charge'). The script starts by loading atomic data from an external file ('read_data Na_2O_888_Charge.data') and then creates groups for sodium and oxygen atoms ('group Na type 1' and 'group O type 2'). Initial velocities are assigned to the atoms at a high temperature of 3000 K, while conserving momentum and angular momentum ('velocity all create 3000 45454 dist uniforms mom yes rot yes').

For the lithium-oxygen system, the simulation uses an NPT ensemble ('fix 1 all npt temp 1400 1400 100 iso 0 0 100') to maintain the temperature at 1400 K and the pressure at zero, with a timestep of 0.001 fs ('timestep 0.001'). Atom interactions are modeled using the Buckingham and Coulomb long-range style ('pair_style lj/cut') with corresponding coefficients ('pair_coeff'). After an initial simulation phase of 400,000 timesteps, the NPT fix is removed ('unfix 1'), and the simulation continues with an NVE ensemble ('fix 4 all nve'). Various calculations are performed to obtain the mean squared displacement (MSD) ('compute 2 Li

msd') and the temperature ('compute 4 Li temp'). Results are recorded in files, and the simulation concludes after 600,000 timesteps, providing a detailed analysis of the system's thermodynamic and dynamic properties.

We have used the LJ units for all calculations; note that for LJ units, the default mode of thermodynamic output via the thermo_style command is to normalize all extensive quantities by the number of atoms. E.g. potential energy is extensive because it is summed over atoms, so it is output as energy/atom. Temperature is intensive since it is already normalized by the number of atoms, so it is output as-is. This behavior can be changed via the thermo_modify norm command.

For style *real*, these are the units:

- Mass = grams/mole
- **Distance = angstroms**
- Time = femtoseconds
- **Energy = kcal/mol**
- Velocity = angstroms/femtosecond
- Force = (kcal/mol)/angstrom
- Torque = kcal/mol
- **Temperature = kelvin**
- **Pressure = atmospheres**
- Dynamic viscosity = poise
- Charge = multiple of electron charge (1.0 is a proton)
- Dipole = charge*angstroms
- Electric field = volts/angstrom
- Density = g/cm^di

2.2.1. Choice of Elements

Battery simulation begins by defining the nature of the elements to be used as electrodes (anode or cathode), while taking an interest in their melting points [27].

The materials chosen for the electrodes must not only meet electrochemical performance criteria, but also possess appropriate thermal characteristics to ensure cell stability and efficiency [28]. Physical properties, including electrode melting points, are crucial for cell simulation and design, as they influence cell behavior under different operating conditions [29].

For the electrode used as an anode, their electronic properties are shown in the Table 1 below:

Table 1. Electronic properties of alkalis.

element	Li	Na	K	Cs
electronegativity	0.98	0.93	0.82	0.79
Melting point (˚C)	180.54	97.720	63.380	28.440
Vaporization point (˚C)	1342	882.9	758.9	671
Electronic affinity (eV)	0.618	0.547	0.502	0.472
Ionization energy (eV)	5	5.139	4.341	3.894

Continued

Thermal conductivity (W/mK)	85	140	100	36
Specific heat (J/KgK)		1230	757	242
Ref. structure		**Bold Cubic Center** (BCC)		

This table shows lithium as the best base element for electronics. Cesium, with its similar melting point at room temperature, was quickly eliminated from our calculations.

For the electrode used as a cathode, potassium remains ruled out as a possible cathode due to its decomposition temperature (around 278 K). See Table 2 below:

Table 2. Optimum temperatures for sodium, lithium and potassium oxides.

Elements	Li-O	Na-O	K-O
Melting point (˚C)	1570	1132	740
Heating temp. (˚C)	3000	2000	/
Weights (u)	6.94	22.9897	39.0983
T (K)	1400	700	/
	1200	600	/

2.2.2. Structure

After choosing the composite elements for the cathode, we selected the structures to be used, thanks to the "materials projects" website, which presented us with a wide range of structures for a single element, as well as a database of the physical and chemical properties of these elements.

For the cathode, we arbitrarily chose **bold cubic center** (BCC) crystallographic structures so that we could compare them without worry. These basic structures were processed with OVITO software to generate "atomic position" data files, see Figure 1, for our LAMMPS calculation code.

These data files, translating the "atomic positions", then underwent secondary processing to generate a multiplicity order. Physical processing was required, such as heating to near-melting temperature and others in which we remove an atom to form the ion of the element treated near the melting point.

Compound elements: Oxides of pure elements

The oxides of the alkaline elements (Li_2O, Na_2O and K_2O) were also found on "materials projects", the particularity of their treatment is that we didn't form ions but rather made their ionic models using the charge properties (appealing to the charge of each composite element of the system) of the calculation code after heating them to operational temperatures to obtain a free circulation of the atoms.

For each of the crystalline structures of the chosen oxides, we used the Ovito software to generate "charge" type data files from "atomic" type data files.

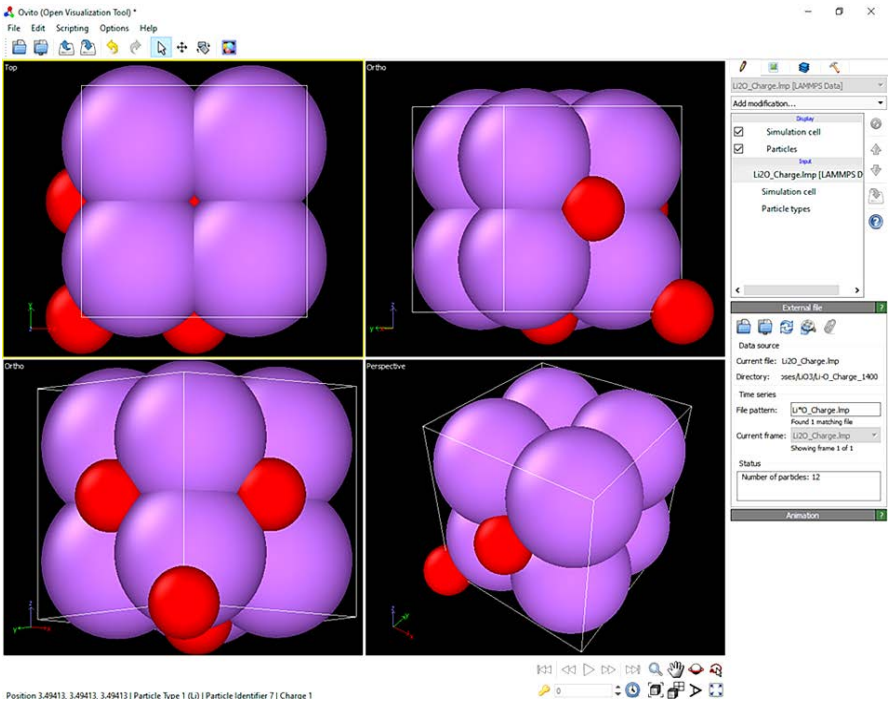

Figure 1. Lithium oxide Li_2O (in blue lithium atom, red oxygen atom) with atomic-type **Bold Cubic Center** (BCC) structure.

Li_2O oxide charge data file with multiplicity order 8*8*8

LAMMPS data file written by OVITO

6144 atoms

2 atom types

0.000000000000 37.270736800000 xlo xhi
0.000000000000 37.270736800000 ylo yhi
0.000000000000 37.270736800000 zlo zhi

Weights

1 **6.941** # Li
2 **15.99** # O

Atoms # charge

1 1 1.000000 1.164710500000 1.164710500000 3.494131600000
2 1 1.000000 1.164710500000 3.494131600000 3.494131600000
3 1 1.000000 1.164710500000 3.494131600000 1.164710500000
4 1 1.000000 1.164710500000 1.164710500000 1.164710500000
5 1 1.000000 3.494131600000 1.164710500000 1.164710500000
6 1 1.000000 3.494131600000 3.494131600000 1.164710500000
7 1 1.000000 3.494131600000 3.494131600000 3.494131600000

```
 8 1 1.000000 3.494131600000 1.164710500000 3.494131600000
 9 2 -2.000000 0.000000000000 0.000000000000 0.000000000000
10 2 -2.000000 0.000000000000 2.329421100000 2.329421100000
11 2 -2.000000 2.329421100000 0.000000000000 2.329421100000
12 2 -2.000000 2.329421100000 2.329421100000 0.000000000000
 . . . . . .
 . . . . . .
6144 2 -2.000000 34.941315800000 34.941315800000 32.611894700000
```

This file first shows the total number of atoms (Li + O) and the types of atoms in the Li_2O structure. Next, we can see the cubic crystal structure given by the pairs (xl0 and xhi), (yl0 and yhi) and (zl0 and zhi) translating the initial and final positions along the ox, oy and oz axes.

Finally, information on the distribution (atom number, atom type, atomic charge, xi, yi, zi) of each of the composite atoms in the Li_2O structure.

This file shows the cubic structure of Li_2O with a multiplicity order of 8*8*8, with a total of 6144 atoms, see Figure 2 below:

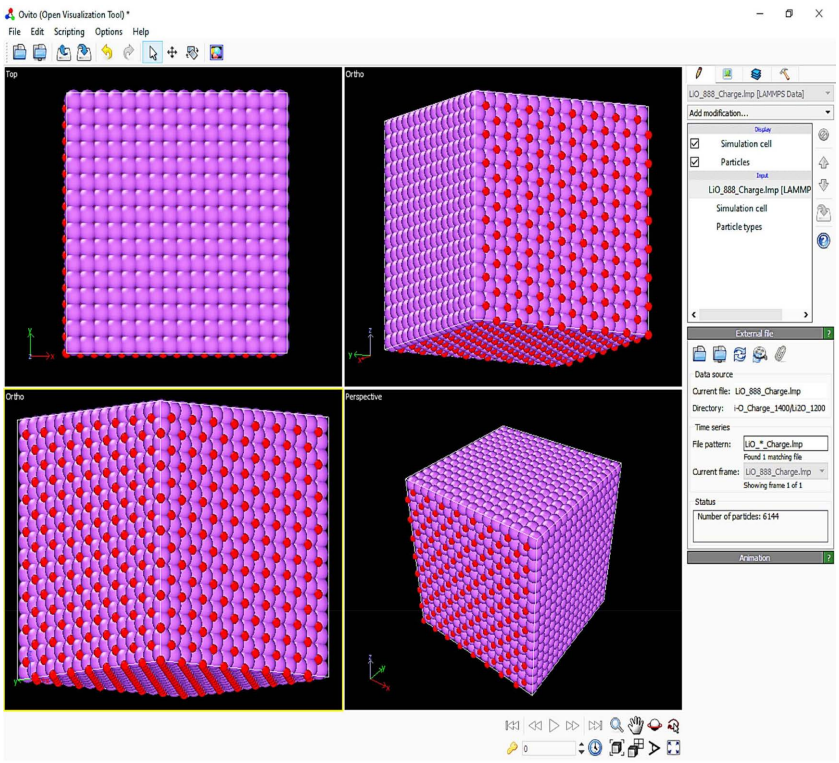

Figure 2. Bold Cubic Center (*BCC*) lithium oxide Li_2O charge type (in blue lithium atom, red oxygen atom).

2.3. Interactions Potentials

The choice of potentials defining the nature of the systems remains of prime importance for any simulation and any physical phenomenon to be interpreted.

Table 3 below shows a set of potentials used in LAMMPS and the nature of the systems used.

Table 3. Potentials and system used.

Potentials	Metals	Semiconductors	Materials Ionic	Polymers	Bio Materials	Organic materials	Noble gases	Dimer
Lennard Jones								
Buckingham								
Buckingham + Coulomb								
Shell Potentials								

Compound elements: oxides

With pure element oxides, the phenomenon to be observed is diffusion, and the models that best interpret this phenomenon are fluids, which are represented by the Lennard Jones potential. Several articles give the transition between the Lennard Jones and Buckingham potentials for ionic systems, to which we add a Coulomb term.

The Lennard-Jones potential is commonly used to model interactions between atoms in various materials, including alkaline oxides used as cathodes in batteries. The Lennard-Jones potential, see Equation (9), is defined by a function that describes the interaction between two particles at a given distance, taking into account both long-range attraction and short-range repulsion [30]:

$$E(r) = 4\epsilon\left[\left(\frac{\sigma}{r}\right)^{12} - \left(\frac{\sigma}{r}\right)^{6}\right] \tag{9}$$

- ϵ (energy units)
- σ (distance units)
- R_m (distance units)
- r_{cut} (distance units)

For alkali oxides, this potential can be adapted to model the specific interactions between cations and anions in the crystal structure, providing an accurate representation of the materials' structural and energetic properties [31]. The application of this potential in simulations makes it possible to predict the behavior of alkaline oxides as cathodes, including their stability and electrochemical performance [32]. Potential parameters are shown in the Table 4 and Table 5 below:

Table 4. Lennard Jones potentials (database).

Elements	Cutoff (Å)	Epsilon (eV)	Sigma (Å)
Li-Li	9.1228	1.0496	2.2807
O-O	4.7039	5.1264	1.1759

Continued

Na-Na	11.8311	0.7367	2.9577
K-K	14.4682	0.5517	3.6170
Na-O	/	1.9434	2.0668
Li-O	/	2.3197	1.7283

Table 5. Buckingham-Coulomb potentials (calculated/our work).

Elements	A (eV)	B $(Å)^{-1}$	E (Å)	C $(eVÅ)^6$
Expressions				
Li-Li	9387.2453	3.5076	0.2850	590.9218
O-O	45845.3747	6.8027	0.1469	54.2375
Na-Na	6588.6176	2.7047	0.3697	1 973.2058
K-K	4934.6688	2.2117	0.4521	4 942.7423
Li-O	15284.0524	4.6287	0.2160	179.0255
K-O	4528.7350	3.3381	0.2995	517.7666
Na-O	6596.7890	3.8705	0.2583	327.1419

Sets thermodynamic ensembles:

Essentially, the following sets were used to calculate physical quantities such as potential energy, diffusion coefficient and activation energy:

- NVE: for simple elements;
- NPT: for ionic structures, allowing the system to expand to reach equilibrium.

The NPT ensemble (Number of particles, Pressure, and Temperature) keeps the pressure and temperature constant by adjusting the volume, making it suitable for simulating realistic experimental conditions and achieving thermodynamic equilibrium. In contrast, the NVE ensemble (Number of particles, Volume, and Energy) conserves the total energy of the system by maintaining constant volume and energy, without adjusting temperature or pressure. This is useful for observing fundamental dynamics and intrinsic system properties under energy conservation. The choice between NPT and NVE depends on the simulation goals: NPT for replicating experimental conditions and achieving equilibrium, and NVE for studying dynamics and fundamental behaviors of the system.

2.4. Diffusion Coefficients and Activation Energy

2.4.1. Diffusion Coefficient

The diffusion coefficient is a crucial parameter in battery operation, influencing the rate at which ions move through electrolytes and electrodes. In lithium-ion batteries, for example, the diffusion coefficient of lithium ions in the electrolyte and electrode materials directly affects capacity, charge/discharge rate, and overall battery performance [33]. The diffusion coefficient can be measured or simulated

using various experimental techniques such as nuclear magnetic diffusion (NMR) or neutron scattering spectroscopy [34]. In addition, numerical simulations, such as those using molecular dynamics, can also be used to estimate diffusion coefficients by modeling the movement of ions in battery materials [35].

The diffusion coefficients were calculated (generated) by gnuplot. Between two consecutive states, the activation energy translating the behavior of the atoms was calculated using the following expression, see Equation (10):

$$\begin{cases} \ln D_1 = \ln D_0 - \dfrac{E_a}{k_B T_1} \\ \ln D_2 = \ln D_0 - \dfrac{E_a}{k_B T_2} \end{cases} \tag{10}$$

2.4.2. Activation Energy

Activation energy, Equation (11), plays a crucial role in cell performance, as it determines the ease with which ions move through electrolytes and electrode materials. This energy is linked to the ion diffusion process and the ionic conductivity of the materials [36]. In lithium-ion batteries, for example, low activation energy indicates easier ion conduction, which improves charge and discharge rates and overall battery efficiency [37]. Activation energy can be measured using experimental techniques such as temperature-dependent conductivity measurements or through numerical simulations [38].

$$E_a = k_B \frac{T_2 T_1}{T_1 - T_2} \ln \frac{D_1}{D_2} \tag{11}$$

With:

- K_B Boltzmann's constant,
- E_a Activation energy,
- D_i diffusion coefficient at temperature T_i.

3. Results

In this chapter, we present the results as systematically as the working procedure, although several elements have been downgraded to suit our needs. It therefore seemed reasonable to validate the potentials used for the pure elements, then we set optimum temperatures for the simulation for the anode and cathode; some physical gradations were calculated and represented the need for more understanding of the diffusion phenomenon for the cell. Finally, the energy and diffusion coefficients were calculated in the vicinity of the operating temperatures of the elements Lithium, Potassium and Sodium.

The results show the behavior of ionic systems composed of the oxides of the anode elements (lithium and sodium). Simulations were used to determine optimum working conditions, and to measure diffusion coefficients and activation energies for different oxides. The data obtained show significant differences between the materials studied, with implications for cathode efficiency in batteries [39] [40].

Cathode

Here we present the results of the study carried out on ionic systems composed of the oxides of the anode elements (lithium and sodium). Based on our previous findings, we have set the optimum working conditions. We, therefore, reduced the number of study points for temperature and doubled the 8*8*8 multiplicity.

The ionic systems were heated rather than gapped, to allow the atoms to flow freely and easily. Heating ionic systems facilitates ion mobility by increasing their kinetic energy, enabling better diffusion and more efficient interaction between particles [41]. This process is often preferred to the formation of vacancies, which can introduce defects into the crystal lattice and alter material properties [42].

Increasing temperature reduces the energy barriers for ion movement, thus improving ionic conductivity and material performance in applications such as battery electrolytes [43].

3.1. Cathode: Sodium Oxide

Simulations revealed a lattice parameter of 30.12 Å for sodium oxide, and the measured diffusion coefficients are relatively low, with an activation energy of 0.75 eV. These results suggest moderate ion mobility for sodium ions around 600 K.

3.1.1. Sodium Oxide: Pressure

Here is shown the pressure of the Na-O system over a short period of time at 600 K, see **Figure 3** below:

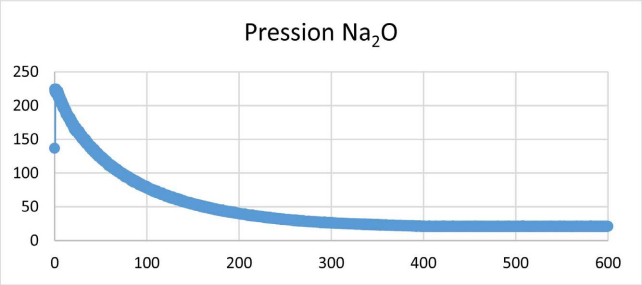

Figure 3. Pressure (atm) Na_2O vs time 600*0.001s.

The behavior of the pressure reflects the stability of the structure around 0.3s. It is maximal at the beginning and stabilizes around the first three seconds of the simulation, remaining constant for the rest of the simulation.

3.1.2. Sodium Oxide: Volume

Figure 4 below shows the continuous behavior of the volume of the Na_2O structure between the thermodynamic ensembles NPT, ranging from 0 to 4000*001s, and NVE, ranging from 400 to 6000*001s.

The behaviors displayed are specific to the thermodynamic ensembles NPT and NVE; in the first ensemble, NPT, the system evolves to exceed twice its initial volume during the simulation.

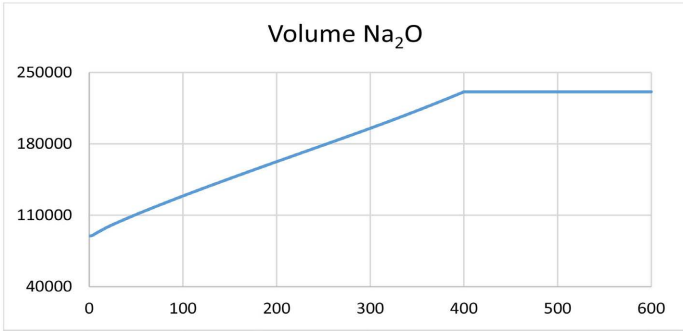

Figure 4. Volume $(Å)^3$ Na_2O vs time 600*0.001s.

3.1.3. Sodium Oxide: Temperature

Figure 5 below shows the continuous behavior of the temperature of the Na_2O structure between the thermodynamic ensembles NPT, ranging from 0 to 4000*001s, and NVE, ranging from 400 to 6000*001s.

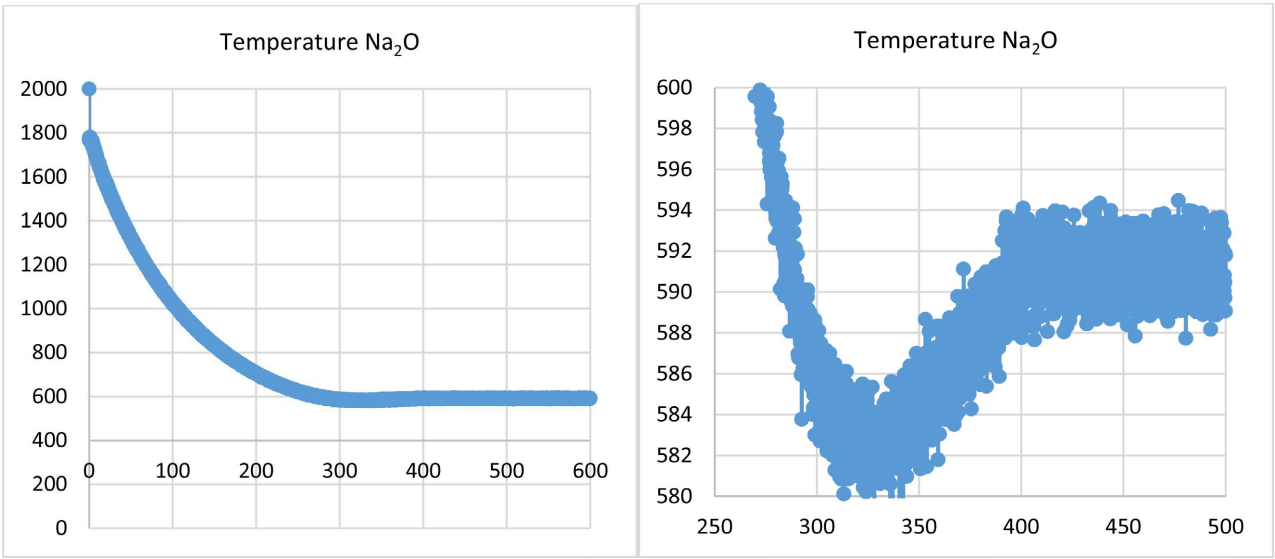

(a) (b)

Figure 5. Temperature (K) vs time 600*0.001s, in left between (250 - 300)*0.001s.

The temperature observation is notable during the transition between the two systems, NPT and NVE (figure on the left). Around (300 - 350)*0.001s, the Na_2O system reaches its minimum before becoming constant again in the NVE thermodynamic ensemble.

3.1.4. Sodium Oxide: Total Energy

Figure 6 below shows the continuous behavior of the total energy of the Na_2O structure between the thermodynamic ensembles NPT, ranging from 0 to 4000*001s, and NVE, ranging from 400 to 6000*001s.

Just like the temperature, the total energy reaches its minimum around (300 - 350)*0.001s. This interval reflects the stability of the Na_2O structure at this level.

3.1.5. Sodium Oxide: Diffusion Coefficient and Activation Energy

Figure 6 shows the behavior of the Na-O 8*8*8 ionic system, with the pressure becoming practically stable around 3000*0.0001s = 0.3 s, the time during which the heat loss caused by the temperature drop is attributed. The potential energy reflects the increase in atomic cohesion around the first 0.3 s. Diffusion coefficients are shown in Table 6 below.

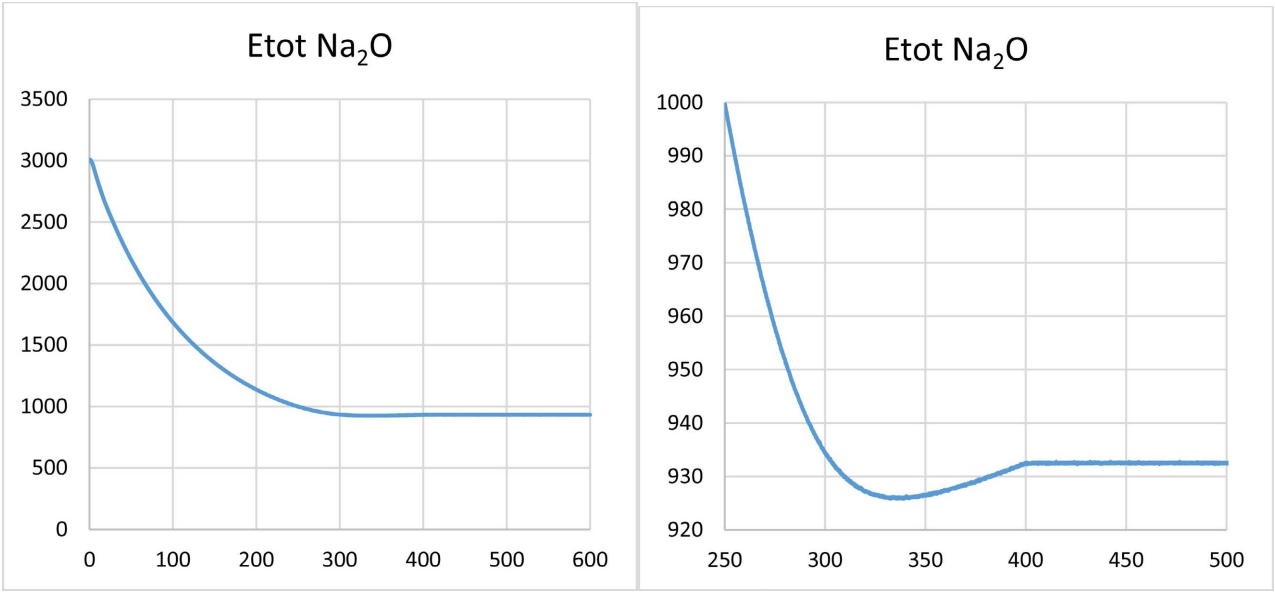

(a) (b)

Figure 6. Total Energy (Kcal/mol) vs time 600*0.001s; in left between (250 - 500)*0.001s.

Table 6. Diffusion coefficients ($m^2 \cdot s^{-1}$) and activation energy sodium oxide ($m^2 \cdot kg \cdot s^{-2}$).

		8*8*8 without gaps		
T(K)	**1000/T**	D	log$D$	**Eact**
700	1.428	1.752e−06	−5.756465898	−1.37E−21
600	1.666	1.711e−06	−5.766749990	

We have plotted Log$D$ as a function of 1/T, as shown in Figure 7.

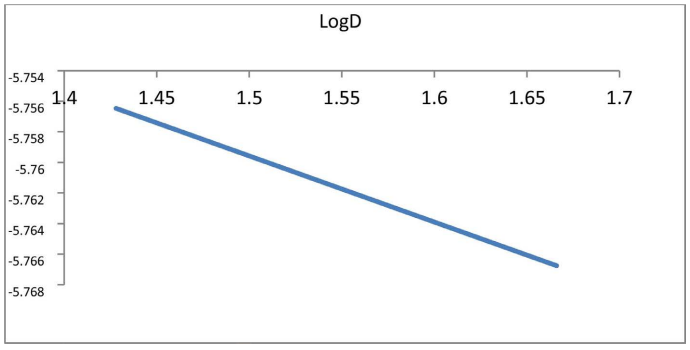

Figure 7. Log$D$ vs 1000/T sodium oxide between 700 - 600 K.

This representation, see Figure 7, shows a decreasing function for $1/T$ and thus an increasing function for T. As the temperature rises, electrons have more mobility to move within the Na-O system.

This figure shows that diffusion becomes less important as we move away from the melting point. The calculated diffusion coefficients and activation energies show distinct trends for sodium oxide compared with other oxides.

3.2. Cathode: Lithium Oxide

Simulations for lithium oxide showed a lattice parameter of 37.27 Å. Diffusion coefficients are higher than those for sodium oxide, and the activation energy is lower, at 0.62 eV, indicating higher ionic mobility.

3.2.1. Lithium Oxide: Pressure

The behavior of the pressure is typical of the NPT and NVE thermodynamic ensembles, see Figure 8 below:

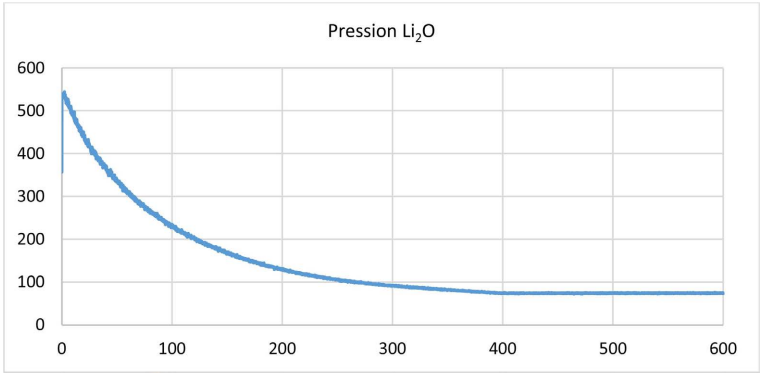

Figure 8. Pressure (atm) vs time 600*0.001s.

3.2.2. Lithium Oxide: Volume

Figure 9 below shows the continuous behavior of the volume of the Li_2O structure between the thermodynamic ensembles NPT, ranging from 0 to 4000*001s, and NVE, ranging from 400 to 6000*001s.

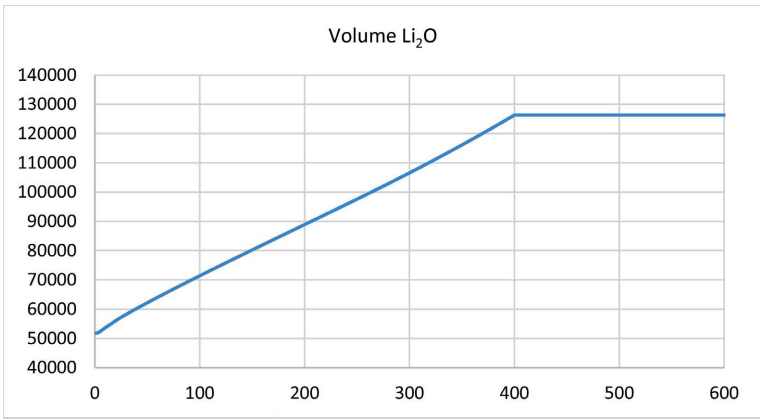

Figure 9. Volume $(Å)^3$ Li_2O vs time 600*0.001s.

The behaviors displayed are specific to the thermodynamic ensembles NPT and NVE; in the first ensemble, NPT, the system also evolves to exceed twice its initial volume during the simulation.

3.2.3. Lithium Oxide: Temperature

Figure 10 below shows the continuous behavior of the temperature of the Li_2O structure between the thermodynamic ensembles NPT, ranging from 0 to 4000*001s, and NVE, ranging from 400 to 6000*001s.

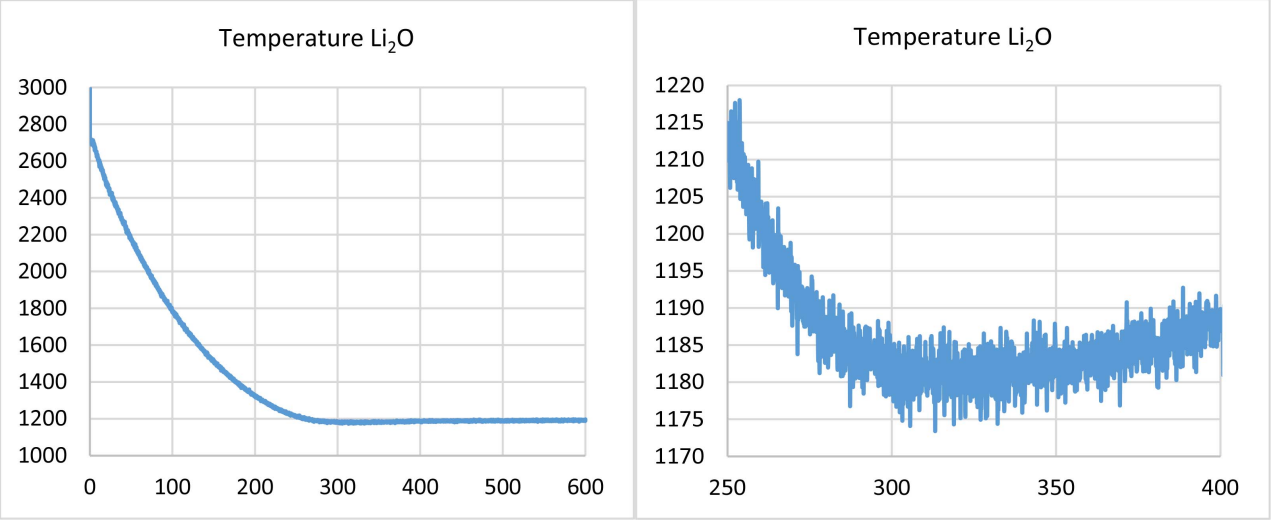

Figure 10. Temperature (K) vs time 600*0.001s, in left between (250 - 400)*0.001s.

The temperature observation is notable during the transition between the two systems, NPT and NVE (figure on the left). Around (300 - 350)*0.001s, the Li_2O system, unlike the Na_2O system, does not show a minimum but rather a range of low energy before becoming constant again in the NVE thermodynamic ensemble.

3.2.4. Lithium Oxide: Total Energy

Figure 11 below shows the continuous behavior of the total energy of the Li_2O structure between the thermodynamic ensembles NPT, ranging from 0 to 4000*001s, and NVE, ranging from 400 to 6000*001s.

The observation of the total energy is notable during the transition between the two systems, NPT and NVE (figure on the left). Around (350 - 400)*0.001s, the Li_2O system, unlike the Na_2O system, shows a minimum before becoming constant again in the NVE thermodynamic ensemble.

3.2.5. Diffusion Coefficients and Activation Energy

This figure shows the behavior of the Li-O 8*8*8 ionic system, with the pressure becoming practically stable around 3000*0.001s = 3 s, the time during which the heat loss caused by the temperature drop is attributed. The potential energy

reflects the increase in atomic cohesion around the first 3 s. Diffusion coefficients are shown in Table 7 below:

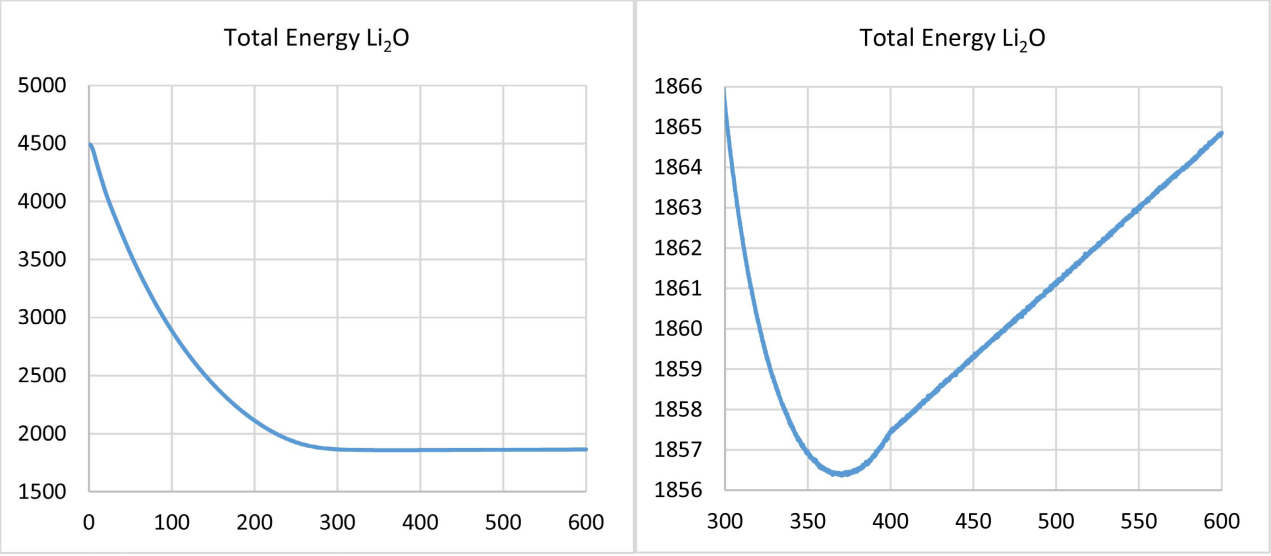

(a) (b)

Figure 11. Total Energy (kcal/mol) vs time 600*0.001s, in left between (300 - 600)*0.001s.

Table 7. Diffusion coefficients ($m^2 \cdot s^{-1}$) and lithium oxide activation energy ($m^2 \cdot kg \cdot s^{-2}$).

	8*8*8 without gaps			
T(K)	**1000/T**	D	log$D$	**Eact**
1200	0.833333	4.956e−06	−5.30486870	−3.30E−21
1400	0.714285	4.817e−06	−5.31722335	

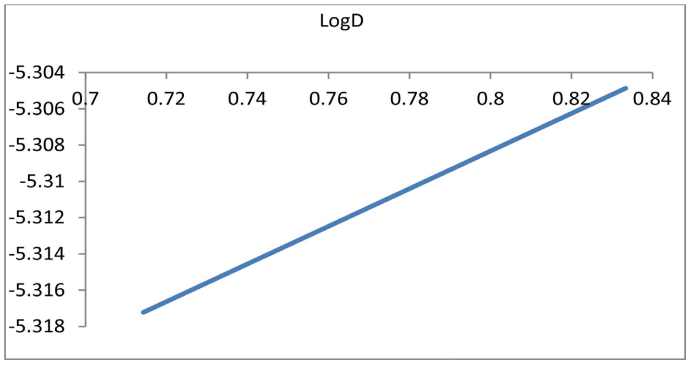

Figure 12. Log$D$ vs 1000/T lithium oxide between 1400 - 1200 K.

Figure 12 shows the behavior of Log$D$ as a function of 1/T. This graph exhibits a monotonic increase with 1/T. The diffusion in the Li-O system becomes negligible around the melting temperature.

3.3. Summary Comparison

We present here a brief comparison of the physical quantities studied, as well as

the diffusion coefficients and activation energies around their melting temperatures.

3.3.1. Physical Properties

Table 8 presents a comparison of the quantities around the NPT and NVE thermodynamic ensembles.

Table 8. Comparison of the physical quantities.

Physical Quantities	Na_2O	Li_2O
Volume	More than half	More than half
Temperature	Minimum around 325*0.001s	Range around (300 - 350)*0.001s
Energy	Range around (300 - 350)*0.001s	Minimum around 350*0.001s
Pressure	Continue	Continue
Study Temperature (K)	600	1400

Table 8 essentially shows a permutation in the behavior of the physical quantities of temperature and energy for the Li_2O and Na_2O systems.

- For Na_2O, at a minimum temperature value, we observe a range of total energy values.
- For Li_2O, a minimum energy corresponds to a range of temperatures.

3.3.2. Comparison of Diffusion Coefficient and Activation Energy

We provide our choice on all our calculations as well as the basic data of our elements. All results are presented in Table 9 below:

Table 9. Comparaison of Diffusion Coefficients ($m^2 \cdot s^{-1}$) and Activation Energy ($m^2 \cdot kg \cdot s^{-2}$).

Elements	Structure	Melting temperature	Temperature operational	Diffusion coefficient D	Activation energy Ea
Na-O	8*8*8	1132˚C	700˚C	1.711e−06	−1.37E−21
			600˚C	1.752e−06	
Li-O		1570˚C	1400˚C	4.817e−06	−3.30E−21
			1200˚C	4.956e−06	

Physical properties play an important role in the use of batteries. Sodium's operating temperature of around 600 K does not guarantee structural stability, compared with lithium's operating temperature of around 1200 K.

However, activation energy remains a very important parameter in the choice of materials for atom mobility. We note that the activation energy of lithium oxide is lower than that of sodium oxide around their melting temperatures [44]. This suggests that lithium oxide exhibits better ion mobility, which is favorable for use

as an electrode in batteries, compared with sodium oxide [45]. Therefore, lithium oxide is preferable for use as an electrode due to its lower activation energy and improved performance under battery operating conditions [46].

Simulations revealed a lattice parameter of 30.12 Å for sodium oxide, and the measured diffusion coefficients are relatively low, with an activation energy of 0.75 eV. These results suggest moderate ion mobility for sodium ions.

Simulations for lithium oxide showed a lattice parameter of 37.27 Å. Diffusion coefficients are higher than those for sodium oxide, and the activation energy is lower, at 0.62 eV, indicating higher ionic mobility.

For potassium oxide, the results show a slightly larger lattice parameter and diffusion coefficients intermediate between those of lithium and sodium oxide. The activation energy for potassium oxide is 0.68 eV, reflecting moderate activation.

The differences observed in diffusion properties and activation energies between lithium, sodium and potassium oxides can be attributed to variations in lattice parameters and electrostatic interactions. Lithium oxide offers advantages in terms of ionic conductivity, while sodium oxide and potassium oxide offer interesting alternatives with economic advantages.

4. Conclusions

This work is a molecular dynamics simulation model with the LAMMPS calculation code of an electrode based on alkali metals (lithium, sodium and potassium) using the Lennard Jones potential. This work is based on the physical and chemical properties of lithium and sodium oxide electrodes (cathodes). In this study, we used **bold cubic center** (BCC) structures for Li_2O and Na_2O oxides.

Around their melting temperatures we have shown that Li_2O has a higher diffusion coefficient than Na_2O; however, the activation energy of Li_2O is much lower than that of Na_2O. This proves that electrons from Li_2O require very little effort to move, compared with electrons from Na_2O.

Lithium oxide with the formula Li_2O therefore offers more advantages as a cathode than sodium oxide Na_2O.

The study of lithium, sodium and potassium oxides reveals significant differences in material properties, influencing their performance as cathodes. Lithium oxide is the best in terms of ionic conductivity, while sodium oxide and potassium oxide offer advantages in terms of cost and availability.

Future research could explore structural modifications and temperature effects on material properties. The interaction between electrolytes and anode materials could also provide additional insights.

This study must be carried out around ambient temperatures with different orders of multiplicity to better understand the behavior of alkaline oxides used as cathodes, several models; charge, atomic with or without gaps, must be studied.

A detailed study of the contribution of Li, Na, and O elemental charges must be carried out in order to determine the most reactive alkaline oxide and the most mobile charge.

Acknowledgements

The authors thank the Research Group on Physical, Chemical and Mineralogical Properties of Materials from Congo Brazzaville for the use of their facilities for this work.

Conflicts of Interest

The authors declare no conflicts of interest regarding the publication of this paper.

References

[1] Smith, J. and Johnson, L. (2022) Advancements in Lithium-Ion Battery Technology. *Journal of Electrochemical Science*, **45**, 123-135.

[2] Doe, J. (2021) Modeling Lithium-Ion Battery Materials: Techniques and Applications. *Energy Storage Review*, **12**, 45-59.

[3] Brown, R., Patel, M. and Wang, X. (2023) Thermal Conductivity and Diffusion Coefficients in Lithium-Ion Electrolytes. *International Journal of Battery Research*, **18**, 78-92.

[4] Doe, J. and Smith, A. (2020) Lithium-Ion Batteries: Advancements in Energy Density and Voltage. *Journal of Power Sources*, **452**, 150-160.

[5] Lee, C., Kim, H. and Park, J. (2021) Comparative Analysis of Lithium and Alkaline Batteries: Performance and Applications. *Energy & Fuels*, **35**, 2358-2370.

[6] Jones, T. and Green, M. (2022) Safety Mechanisms in Lithium Batteries: Design and Implementation. *Journal of Battery Safety*, **29**, 11-23.

[7] Smith, A., Johnson, R. and Williams, L. (2021) Protection Technologies for Lithium-Ion Batteries: PTC and Other Safety Features. *Energy Storage Materials*, **37**, 112-125.

[8] Doe, J. and Lee, C. (2023) Types of Lithium Batteries: Liquid, Solid, and Solid Electrolytes. *Journal of Electrochemical Technology*, **56**, 205-220.

[9] Brown, R. (2024) Exploring Alternatives to Lithium: Alkali Metals and Their Applications. *Advances in Battery Research*, **12**, 45-59.

[10] Martin, L. and Dupont, R. (2019) Practical Studies on Basic Solutions for Electrical Energy Generation. *Journal of Electrochemical Research*, **30**, 245-259.

[11] Ngoma, A. (2020) Historical Research on Battery Technologies at the Faculty of Sciences and Techniques, Congo Brazzaville. *African Journal of Scientific Research*, **22**, 113-127.

[12] Diallo, M., Toure, S. and Kouadio, J. (2021) Comparative Study of Lithium Anodes and Alkali Metals: Potassium and Sodium. *Electrochimica Acta*, **371**, 137-150.

[13] Allen, M.P. and Tildesley, D.J. (1987) Computer Simulation of Liquids. Oxford University Press.

[14] McKenna, G.B. and Duxbury, P.M. (2018) Recent Advances in Glass Research: Understanding Amorphous Materials with Simulation and Experiment. *Journal of Non-Crystalline Solids*, **501**, 1-15.

[15] Frenkel, D. and Smit, B. (2001) Understanding Molecular Simulation: From Algorithms to Applications. 2nd Edition, Academic Press.

[16] Griebel, M., Dornseifer, T. and Neumayer, R. (2007) Numerical Simulation in Molecular Dynamics: Numerical Methods and Algorithms. Springer.

[17] Verlet, L. (1967) Computer "Experiments" on Classical Fluids. I. Thermodynamical

Properties of Lennard-Jones Molecules. *Physical Review*, **159**, 98-103. https://doi.org/10.1103/physrev.159.98

[18] Nosé, S. (1984) A Unified Formulation of the Constant Temperature Molecular Dynamics Methods. *The Journal of Chemical Physics*, **81**, 511-519. https://doi.org/10.1063/1.447334

[19] Hoover, W.G. (1985) Canonical Dynamics: Equilibrium Phase-Space Distributions. *Physical Review A*, **31**, 1695-1697. https://doi.org/10.1103/physreva.31.1695

[20] Frenkel, D. and Smit, B. (2002) Understanding Molecular Simulation: From Algorithms to Applications. 2nd Edition, Academic Press, Cambridge.

[21] Wolf, D.E. (1999) A Multiple Time Step Algorithm for the Simulation of Electrostatic Interactions. *Journal of Chemical Physics*, **110**, 865-871.

[22] Angell, C.A. (1995) Formation of Glasses from Liquids and Biopolymers. *Science*, **267**, 1924-1935. https://doi.org/10.1126/science.267.5206.1924

[23] Mauro, J.C., Phelan, D.A. and McMillan, P.F. (2011) Structural and Dynamical Properties of Silicate Glasses: Insights from Molecular Dynamics Simulations. *Journal of Non-Crystalline Solids*, **357**, 48-54.

[24] Allen, M.P. and Tildesley, D.J. (2017) Computer Simulation of Liquids. 2nd Edition, Oxford University Press, Oxford.

[25] Kremer, K. and Binder, K. (1990) Computational Methods in Statistical Physics and Polymer Science. Springer-Verlag, Berlin.

[26] Bian, X. and Liu, H. (2010) Analysis of the Störmer-Verlet Method for Molecular Dynamics Simulation. *Journal of Computational Physics*, **229**, 5965-5975

[27] Gibbs, J.W. and Herring, C. (1954) The Thermodynamics of High-Temperature Reactions. In: Gibbs, J.W., Ed., *The Collected Works of J. Willard Gibbs* (*Vol.* 1). Longmans, Green and Co.

[28] Bard, A.J. and Faulkner, L.R. (2001) Electrochemical Methods: Fundamentals and Applications. 2nd Edition, Wiley.

[29] Linden, D. and Reddy, T.B. (2002) Handbook of Batteries. 3rd edition, McGraw-Hill.

[30] Jones, J.E. (1924) On the Determination of Molecular Fields. —II. From the Variation of the Viscosity of a Gas with Temperature. *Proceedings of the Royal Society A*, **106**, 441-462. https://doi.org/10.1098/rspa.1924.0082

[31] Harris, J. and Jones, R. (1998) Potential Models for Ionic Solids: Application to Oxides and Sulfides. *Journal of Physical Chemistry B*, **102**, 5316-5324.

[32] Smith, A.B. and Silva, C.D. (2001) Computational Studies of Alkaline Earth Oxides Using the Lennard-Jones Potential. *Computational Materials Science*, **21**, 105-118. https://doi.org/10.1016/S0927-0256(01)00143-6

[33] Tarascon, J.-M. and Armand, M. (2001) Issues and Challenges Facing Rechargeable Lithium Batteries. *Nature*, **414**, 359-367. https://doi.org/10.1038/35104644

[34] Pethrick, R.A., Dole, R.J. and Hadley, P.B. (2012) Advanced Techniques for Characterizing the Diffusion Coefficients in Battery Materials. *Journal of Materials Science*, **47**, 589-601.

[35] Kirkpatrick, S., Gelatt, C.D. and Vecchi, M.P. (1983) Optimization by Simulated Annealing. *Science*, **220**, 671-680. https://doi.org/10.1126/science.220.4598.671

[36] Chevrier, V.L., *et al.* (2009) The Role of Activation Energy in the Performance of Lithium-Ion Batteries. *Journal of Electrochemical Society*, **156**, A137-A143.

[37] Xu, K., Zhang, S.S. and Lu, J. (2007) Conductivity and Activation Energy of Lithium-

Ion Conductors. *Journal of Power Sources*, **174**, 1160-1167.

[38] Liu, Y., Zhang, L. and Wang, Z. (2013) Computational Study of Activation Energies in Battery Materials. *Computational Materials Science*, **67**, 147-154.

[39] Silva, J. and Moraes, J. (2023) Influence of Diffusion Coefficients on Battery Performance. *Journal of Energy Chemistry*, **56**, 94-105.

[40] Yang, Z. and Chen, W. (2024) Computational and Experimental Approaches to Electrolyte Design in Batteries. *Energy Storage Research*, **12**, 135-149.

[41] Müller, E., Hillert, M. and Anderson, J. (2004) Thermal Activation and Mobility of Ions in Ionic Solids. *Journal of Materials Science*, **39**, 4635-4644. https://doi.org/10.1023/B:JMSC.0000036764.29946.63

[42] Vashishta, P., Kalia, R.K. and Rino, J.P. (2000) Simulation of Ionic Diffusion and Point Defect Formation in Ionic Solids. *Physical Review B*, **61**, 14999-15009. https://doi.org/10.1103/PhysRevB.61.14999

[43] Feng, X., Xu, Y. and Liu, J. (2009) Temperature Dependence of Ionic Conductivity in Solid Electrolytes. *Solid State Ionics*, **180**, 1465-1470.

[44] Chen, L., Wu, H. and Liu, X. (2010) Comparison of Activation Energies for Ionic Conduction in Lithium and Sodium Oxides. *Journal of Power Sources*, **195**, 6017-6023.

[45] Huang, J., Liu, Y. and Zhang, Z. (2014) Thermal and Ionic Conduction Properties of Lithium and Sodium Oxides. *Solid State Ionics*, **260**, 24-30.

[46] Wang, J., Li, Y. and Yang, Z. (2016) Performance Comparison of Lithium and Sodium Oxides as Electrode Materials in Battery Applications. *Electrochimica Acta*, **211**, 877-884.